Control Strategy for Battery/Flywheel Hybrid Energy Storage in Electric Shipboard Microgrids

Jun Hou, *Member, IEEE*, Ziyou Song, *Member, IEEE*, Heath Hofmann *Senior Member, IEEE*, and Jing Sun, *Fellow, IEEE*

***Abstract*—Integrated power system (IPS) combines electrical power for both ship service and electric propulsion loads by forming a microgrid. In this paper, a battery/flywheel hybrid energy storage system (HESS) is studied to mitigate load fluctuations in a shipboard microgrid. This paper focuses on how to determine the reference operation state of the flywheel, which depends on both future power load and the power split between the battery and flywheel. Two control strategies are proposed: an optimization-based approach and a lookup-table-based approach. Case studies are performed in different sea conditions, and simulation results demonstrate that the proposed control strategies outperform baseline control strategies in terms of power fluctuation mitigation and HESS power loss reduction. A comparison between the two proposed approaches is performed, where their performances are quantified, the advantages and disadvantages of each strategy are analyzed, and the cases where they are most applicable are highlighted.**

***Index Terms*—Shipboard Microgrid; Battery and Flywheel Hybrid Energy Storage; Power Fluctuation Mitigation; Model Predictive Control.**

I. Introduction

INTEREST in microgrid systems has increased as they are required for considerable systems and services [1]. Energy sources (such as turbines, fuel cells, and solar panels), as well as energy storage (such as batteries, flywheels, and ultra-capacitors), interact with the electric loads of the microgrid system [2], [3]. In microgrid systems, smoothing power fluctuations is important to maintaining system reliability and improving efficiency [4]. Energy storage systems (ESS), including batteries, flywheels, and ultra-capacitors, are an effective solution, and typically work as a buffer to compensate these fluctuations [5]. Given their high energy density, batteries have been a common solution to smoothing power fluctuations in microgrids [6]. However, due to the limitations of Li-Ion batteries, such as cycle life and power density [7], a hybrid energy storage system (HESS) consisting of multiple energy storage provides a more robust and cost-efficient solution.

This paper focuses on shipboard microgrid systems for all-electric ships, which have become a dominant trend for both commercial and military ship development to improve efficiency, support high-power mission systems, reduce emissions, and provide a more comfortable environment [8]–[11]. However, because of the propeller rotation and encountered waves, the resulting load fluctuations can significantly affect both the mechanical and electrical systems [12]. In order to address this issue, one solution is to incorporate an ESS to smooth the load power [13], [14]. Compared to using one single type of ESS, different combinations of ESSs, namely HESS, can improve the system performance in terms of size, weight, and cost for an electric ship. [15]. Flywheels have been used as uninterruptible power supplies (UPS) [16], and for wind power smoothing [17] and stationary power systems [18]. The development of magnetic bearings, resulting in significantly reduced friction losses, has facilitated high-speed flywheels and made them more attractive for a wide range of applications [19]. For electrified ships, the role of flywheel technology has been mentioned in the US Naval Power System Technology Development Roadmap [20]. In general, flywheels have high power density, long lifetime (in both calendar life and cycle life), and a superior ability to operate over a much wider temperature range when compared to batteries [19]. However, they have lower energy density and higher standby losses. Given their complementary characteristics, a battery combined with flywheel (B/FW) HESS is studied in this paper to address propulsion-load fluctuations on the shipboard microgrid. Control strategy is essential to achieve the effectiveness of the B/FW HESS. In this work, we explore model predictive control (MPC) based control strategies due to its capability in dealing with constraints and achieving optimal solutions [21], [22]. Given the nonlinear nature of flywheel dynamics, the computational intensity involved with the MPC will make it computationally intensive. Using a short predictive horizon is one way to reduce the computational burden of MPC, but it usually has a negative consequence in performance.

In this paper, we address the challenge of B/FW HESS energy management with short horizon MPC combined with flywheel state of charge (SOC) planning. The SOC reference is intended to provide an optimal operating point for energy storage, so that the MPC can focus on short-horizon power tracking. The reasons why only flywheel SOC planning is considered are discussed in the following. The energy density of Li-ion batteries is much higher than that of flywheels; and in nominal conditions, flywheels are more efficient than batteries [23]. Moreover, temperature and aging have significant impacts on battery capacity and internal resistance [24]. The internal resistance of the battery can increase by over

Manuscript received December 21, 2019; accepted January 16, 2020. Paper no. TII-19-5427(Corresponding author: Ziyou Song.)

Jun Hou and Heath Hofmann are with the Department of Electrical Engineering and Computer Science, Ziyou Song and Jing Sun are with the Department of Naval Architecture and Marine Engineering, University of Michigan, Ann Arbor, Michigan 48109 USA (e-mail: junhou@umich.edu; ziyou@umich.edu; hofmann@umich.edu; jingsun@umich.edu).

100% due to low temperature and battery aging [25]. Given the high efficiency of flywheels, more fluctuations will be compensated by the flywheel, leading to more usage of the flywheel. Therefore, the SOC variation of the battery will be smaller than that of the flywheel. Furthermore, compared to the flywheel, at the nominal temperature (15C-35C), the efficiency of the battery is insensitive to its SOC variation during the operation range [25], [26], namely 20%-90% in this study. Therefore, flywheel SOC planning is used to improve the performance of a short predictive horizon MPC, and the battery will be used to maintain the flywheel operating at its reference SOC. SOC planning of the battery for plug-in hybrid electric vehicles (PHEVs) via vehicle-to-vehicle (V2V) connectivity has been investigated in [27]. The whole trip information [28] is required to plan the optimal battery SOC trajectory globally. Cloud computing and V2V connectivity are used to achieve this goal. However, this might not be available, and so is not considered in this study. To the best of our knowledge, flywheel SOC planning has not been explored well. Reference [17] investigates flywheel SOC planning for wind power smoothing. In [17], a lookup table, which is pre-calculated by an optimization routine designed to minimize the losses of the flywheel at different power loads, is used to generate the SOC reference. The mean value of forecasted power loads (over a 10-minute horizon) is utilized as the input of this lookup table. However, this approach might not be suitable for our application for the following reasons. First of all, it is difficult to predict future loads for a long horizon (such as 10 minutes), because the propulsion-load fluctuations are related to not only encountered waves, but also the operation of the ship. As the predictive horizon increases, the predictive errors become larger. Furthermore, a power split between battery and flywheel must be taken into consideration for HESS. Additionally, the mean value is not an indication of the power associated with load fluctuations.

In order to provide effective SOC planning of the flywheel with a short predictive horizon, a novel control strategy, which integrates MPC with an SOC planning approach, is developed in this paper. A lookup-table based approach, which uses the mean value of the future power from MPC, is developed as a baseline control strategy for performance evaluation and analysis. This approach is similar to the one in [17]. Because the mean value does not represent the power associated with load fluctuations, another lookup-table based approach is developed to use instantaneous power loads as inputs to the lookup table for the SOC reference calculation. We propose two different flywheel SOC planning approaches. One uses the root mean square (RMS) power, instead of the mean power, as the input for the SOC-reference determination, as it better represents the power associated with load fluctuations. The other is an optimization-based approach, which is developed to integrate SOC planning with power tracking and loss minimization. A comparison study is performed to compare the proposed approaches with the baseline approach. Furthermore, the advantages and limitations of the proposed approaches are discussed. A hardware-in-the-loop test has been performed to demonstrate the real-time feasibility of the MPC approach. The main contributions of this paper are summarized as follows:

- A novel optimization-based SOC-planning approach is developed and combined with MPC. The outputs of MPC, which take the power split into consideration, are used to determine the flywheel SOC reference. This SOC-planning approach is effective to address issues caused by a short predictive horizon of MPC, leading to the mitigation of load fluctuations and improved energy efficiency.
- RMS power, instead of mean power, is used for the proposed lookup-table-based approach to obtain the flywheel SOC reference. Note that the optimization-based approach is more suitable when the controller hardware capability is sufficient; otherwise, the lookup-table-based approach using RMS power is preferred.

This paper is organized as follows. The system description and problem formulation are presented in Section II. Models of the propeller/ship dynamics and B/FW HESS are also introduced. In Section III, four different SOC-planning approaches to obtain the flywheel SOC reference are developed. In Section IV, comparison results are presented and analyzed. Section V concludes the paper.

II. System Description and Problem Formulation

In this paper, Medium voltage DC (MVDC) power generation is considered as the architecture of the shipboard microgrid, where the prime mover and generator (PM/G) sets, the B/FW HESS, and the propulsion motor(s) are connected to the DC bus, as shown in Fig. 1. The PM/G sets provide the average power to the DC bus, and the motor drives the propeller to generate the thrust for the ship. The B/FW HESS works as an energy buffer to absorb power when the motor is under-loaded and supply power when over-loaded, therefore mitigating the propulsion-load fluctuation effects. Because of the encountered waves (relatively low frequency) and the rotational motion of the propeller (relatively high frequency), the propulsion-load fluctuations contain multi-frequency components associated with wave frequencies and propeller speed. Furthermore, if the propeller is in-and-out-of water, additional frequency components will be included in the load fluctuations. Through the mechanical connection between the motor and the propeller, the reliability and efficiency of the shipboard microgrid can be affected by these fluctuations.

In this section, a dynamic model of an electric ship propulsion system with B/FW HESS is presented. Following that, the MPC problem formulation is developed. The research challenge of obtaining the optimal flywheel SOC reference is analyzed at the end of this section.

A. Propeller and Ship Dynamic Model

The propeller and ship dynamic model was developed in [14] and is summarized in this section for easy reference.

The propulsion-load power is expressed as:

$$P_{Load} = 2\pi n Q, \tag{1}$$

where Q is the load torque generated by the propeller, n is the propeller rotational speed in revolutions-per-second, and the motor speed is assumed to be the same as propeller speed. The propeller output torque is presented as:

This article has been accepted for publication in a future issue of this journal, but has not been fully edited. Content may change prior to final publication. Citation information: DOI 10.1109/TII.2020.2973409, IEEE Transactions on Industrial Informatics

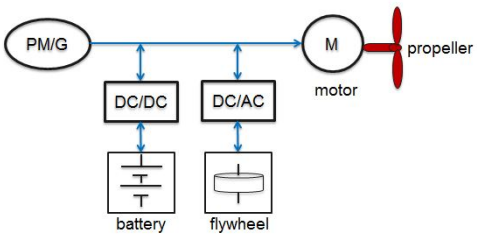

Figure 1: The overall structure of the B/FW HESS in the shipboard network.

$$Q = \mathrm{sgn}(n)\beta K_{Q0}\rho n^2 D^5, \tag{2}$$

where β is the in-and-out-of-water loss factor, K_{Q0} represents the torque coefficient without in-and-out-of-water behavior, ρ is the water density, and D is the propeller diameter. The torque coefficient K_{Q0} is a function of ship speed, advance ship speed, and wake field. Note that this model is able to capture the propeller and ship dynamics. The detailed dynamic equations can be found in [14].

B. Hybrid Energy Storage System Model

The state of charge (SOC) of the batteries and flywheels are defined as the state variables. The flywheel SOC is determined as $SOC_{FW} = \frac{\omega}{\omega_{max}} \times 100\%$ [29], where ω and ω_{max} are the current and maximum speeds of the flywheel, respectively. The SOC of the battery is expressed as $SOC_B = \frac{Q_{battery}}{Q_B} \times 100\%$, where $Q_{battery}$ and Q_B are the current and maximum capacities of the battery, respectively. The battery current and flywheel torque are defined as the control variables. The HESS model is described in the following:

$$\begin{aligned} \dot{SOC}_B &= -\frac{1}{3600 Q_B} I_B, \\ \dot{SOC}_{FW} &= -\frac{b}{\omega_{max} J_{FW}} SOC_{FW} - \frac{1}{\omega_{max} J_{FW}} T_{FW}, \end{aligned} \tag{3}$$

where b, J_{FW}, and T_{FW} are the drag coefficient, inertia, and torque of the flywheel, respectively. The energy losses and output powers of battery and flywheel modules are presented in the following:

$$\begin{aligned} &Loss_B = N_B R_B I_B^2, \\ &Loss_{FW} = N_{FW}\left[\frac{3}{2} R_s \left(\frac{T_{FW}}{\frac{3}{4} p_{PM} \Lambda_{FW}}\right)^2 + b(\omega_{max} SOC_{FW})^2\right], \\ &P_B = N_B V_{OC}(SOC_B) I_B - Loss_B, \\ &P_{FW} = N_{FW}\omega_{max} SOC_{FW} T_{FW} - Loss_{FW}, \end{aligned} \tag{4}$$

where N_{FW} and N_B are the number of flywheel and battery modules, respectively; R_B and $V_{OC}(SOC_B)$ are the battery equivalent series resistance (ESR) and open-circuit voltage; p_{PM}, R_s and Λ_{FW} are the number of poles, the stator resistance, and the permanent magnet (PM) flux linkage of the PM motor/generator. The losses of HESS include conduction losses and standby losses. In (4), $R_B I_B^2$ and $\frac{3}{2} R_s \left(\frac{T_{FW}}{\frac{3}{4} p_{PM} \Lambda_{FW}}\right)^2$ are the conduction losses of the battery and flywheel, respectively. In general, the standby losses of batteries [35] can be ignored, but the standby losses of high-speed flywheels, due to the spinning, cannot be neglected [36]. In this model, the standby loss of the flywheel is captured by $b(\omega_{max} SOC_{FW})^2$, which includes windage loss and core loss [29]. The flywheel motor/generator is controlled to operate at its minimum current operating point to reduce losses.

Table I: Battery parameter identification results within 20%-90% SOC at 25^oC.

	R_0	R_1	$\tau(RC)$
[26]	9-9.5$m\Omega$	21.3-75$m\Omega$	431-1104sec
[30]	0.45-0.5Ω	0.02-0.03Ω	25-40sec
[31]	2$m\Omega$	2$m\Omega$	100sec
[32]	2-2.35$m\Omega$	1.8-2.5$m\Omega$	32-40sec
[33]	2$m\Omega$	0.9-1$m\Omega$	28-42sec
[34]	0.1Ω	0.03-0.01Ω	25-28sec
[35]	0.1062Ω	0.0523Ω	23.21sec
This paper	60$m\Omega$	187$m\Omega$	59sec

In general, a first-order equivalent circuit model (ECM) can capture the battery dynamics sufficiently. The parameters of the first-order ECM have been studied by many researchers. The identification results, including the battery used in this paper, are summarized in Table I. In general, the RC time constant of a battery is from tens of seconds to hundreds of seconds. As shown in Table I, the RC time constant of our battery pack is about 60 sec. The RC time constant is much longer than the control horizon (0.02 sec) and the predictive horizon (0.2 sec; $N_T = 10$). Furthermore, the frequencies of load fluctuations are also much higher than that of the RC pair. Therefore, the RC pair has only a slight influence on the MPC performance. Because the RC pair will introduce another state into MPC, leading to increased computational cost, a control-oriented HESS model with only one equivalent series resistance is used in the paper. In order to evaluate the control strategies, the first-order equivalent circuit model is used in the simulation. Note that the internal resistance of the battery changes with the battery SOC, temperature, and aging [24], [25]. However, the time scales of these effects are much longer than the RC time constant. Therefore, within the predictive horizon, the internal resistance of the battery can be assumed to be constant, and online parameter identification can update the battery resistance accordingly.

C. Model Predictive Control Formulation

Compensating load fluctuations and reducing HESS losses to improve system reliability and efficiency are two primary objectives of the energy management strategy. Two cost functions can be used to capture these objectives:

$$J_1 = \sum_{k=t}^{t+N_T T_s} (P_{FL}(k) - P_{HESS}(k))^2, \tag{5}$$

$$J_2 = \sum_{k=t}^{t+N_T T_s} (P_{HESS_{Loss}}(k)), \tag{6}$$

This article has been accepted for publication in a future issue of this journal, but has not been fully edited. Content may change prior to final publication. Citation information: DOI 10.1109/TII.2020.2973409, IEEE Transactions on Industrial Informatics

where $N_T T_s$ is the optimization window, T_s is the sampling time, P_{FL} is the power of load fluctuations; P_{HESS} is the output power of HESS; and $P_{HESS_{Loss}} = Loss_B + Loss_{FW}$ represents the power loss of the HESS. Because $N_T T_s$ is constant, minimizing J_1 is equivalent to minimizing the RMS tracking error. Future load fluctuations can be predicted by model-based approaches or data-based approaches. One approach for the prediction of the future load information has been published in [5]. As the prediction of the future load fluctuations is not the focus of this paper, we assume that this prediction is known.

Reducing the tracking error could lead to increased HESS losses and vice versa, so the multi-objective optimization problem (MOP) of minimizing J_1 and J_2 has no single optimal solution. In this paper, the MOP is converted to a single-objective optimization problem using then weighted-sum method:

$$J_{HESS} = \sum_{k=t}^{t+N_T T_s} (1-\lambda)(P_{FL}(k) - P_B(k) - P_{FW}(k))^2 + \lambda(Loss_B(k) + Loss_{FW}(k)), \quad (7)$$

subject to the constraints:

$$\begin{aligned} SOC_{B,min} \le SOC_B \le SOC_{B,max}, \\ SOC_{FW,min} \le SOC_{FW} \le SOC_{FW,max}, \\ I_{B,min} \le I_B \le I_{B,max}, \\ T_{FW,min} \le T_{FW} \le T_{FW,max}, \\ P_{FW,min} \le T_{FW} SOC_{FW} \omega_{max} \le P_{FW,max}, \end{aligned} \quad (8)$$

$$\begin{bmatrix} SOC_B(k+T_s) \\ SOC_{FW}(k+T_s) \end{bmatrix} = \begin{bmatrix} 1 & 0 \\ 0 & 1 - \frac{bT_s}{\omega_{max} J_{FW}} \end{bmatrix} \begin{bmatrix} SOC_B(k) \\ SOC_{FW}(k) \end{bmatrix} - \begin{bmatrix} \frac{T_s}{3600 Q_B} & 0 \\ 0 & \frac{T_s}{\omega_{max} J_{FW}} \end{bmatrix} \begin{bmatrix} I_B(k) \\ T_{FW}(k) \end{bmatrix}, \quad (9)$$

where $0 \le \lambda \le 1$ is the weighting factor that allows us to put different emphasis on each attribute to investigate the performance trade-off. Equation (9) is obtained by discretizing (3) using $T_s = 0.02sec$. The sampling time is chosen based on the system dynamics, where the high-frequency fluctuation is around 8Hz. A high sampling rate increases the computational cost, so that the sampling rate is chosen to be a reasonably value, i.e., 50Hz. In this study, the upper and lower boundaries of the battery and flywheel are chosen $SOC_{B,min} = 20\%$, $SOC_{B,max} = 90\%$, $SOC_{FW,min} = 30\%$, $SOC_{FW,max} = 99\%$, $I_{B,min} = -200A$, $I_{B,max} = 200A$, $T_{FW,min} = -40Nm$, $T_{FW,max} = 40Nm$, $P_{FW,min} = -90kW$, and $P_{FW,max} = 90kW$. In marine applications, a longer self-sustained operation time, which is defined as the time interval that the HESS does not require charging or discharging from external power sources, such as a diesel generator, could offer a more flexible schedule for the generator sets, thereby resulting in a better system efficiency. In this paper, the self-sustained operation time is chosen to be 40 minutes. If the entire self-sustained operation period is used as the optimization window, (7) would be solved for N=120,000, making the optimization problem computationally prohibitive for real-time applications [37]. Alternatively, a receding-horizon based MPC formulation is developed for real-time applications. An MPC with a short predictive horizon, however, cannot incorporate long-term aspects of the operation.

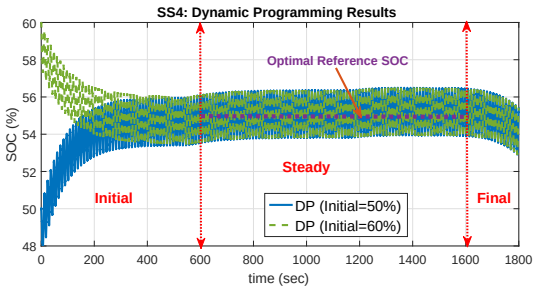

Figure 2: Global optimization solutions with different initial SOCs determined using dynamic programming.

In order to illustrate the issue of MPC with a short predictive horizon, a theoretical analysis is performed. Several assumptions are made in order to provide an analytical solution: the predictive horizon $N_T = 1$; $N_B V_{OC} I_B \gg Loss_B$ and $N_{FW} \omega_{FW} T_{FW} \gg Loss_{FW}$; the load fluctuations are fully compensated by the HESS ($P_{FL}(k) = P_{HESS}(k)$); and the constraints are inactive. Then the cost function can be simplified as:

$$J(k) = N_B R_B I_B^2(k) + N_{FW}(R_{FW} T_{FW}^2(k) + b\omega_{FW}^2(k+T_s)), \quad (10)$$

where $P_{FL}(k) = P_{HESS}(k)$ and $R_{FW} = \frac{3}{2} R_s \frac{1}{\frac{3}{4} p_{PM} \Lambda_{FW}}^2$. Since $\omega_{FW}(k)$ is the speed at time k, the cost function minimizes the standby loss $b\omega_{FW}^2(k+T_s)$, instead of $b\omega_{FW}^2(k)$. According to the assumption, the battery current I_B can be represented by T_{FW} and P_{FL}: $I_B = \frac{P_{FL} - N_F \omega_{FW} T_{FW}}{N_B V_{OC}}$. The optimal solution of T_{FW} can be obtained by solving $\frac{\partial J(k)}{\partial T_{FW}(k)} = 0$:

$$T_{FW} = \frac{R_B J_{FW}^2 \omega_{FW} P_{FL} + (J_{FW} - bT_s) bT_s N_B V_{OC}^2 \omega_{FW}}{N_{FW} R_B J_{FW}^2 \omega_{FW}^2 + N_B V_{OC}^2 (R_{FW} J_{FW}^2 + bT_s^2)}. \quad (11)$$

Because $(J_{FW} - bT_s) > 0$ and $\omega_{FW} > 0$, there always exists a discharge component in T_{FW} to decrease the flywheel rotational speed. Furthermore, the drag term $b\omega_{FW}$ also decreases the rotational speed. Since P_{FL} is a periodic fluctuating term, the flywheel speed will continuously decrease with oscillations until reaching the minimum speed constraint. When the flywheel reaches the minimum speed constraint, the HESS essentially becomes a battery system, leading to poor performance in terms of both the fluctuation compensation and HESS loss reduction. In order to consider the whole self-sustained operation time, in contrast, global optimization solutions with different initial flywheel SOCs are obtained using dynamic programming, as shown in Fig. 2, where the flywheel operates around an optimal reference SOC (speed) in steady-state to achieve a high system efficiency.

To keep the flywheel operating in a high-efficiency range without extending the predictive horizon, a penalty on the SOC deviations from the defined flywheel SOC reference $\gamma(SOC_{FW}(k) - SOC_{FW_d})^2$ is added into the cost function. The MPC for the B/FW HESS is then expressed as follows:

This article has been accepted for publication in a future issue of this journal, but has not been fully edited. Content may change prior to final publication. Citation information: DOI 10.1109/TII.2020.2973409, IEEE Transactions on Industrial Informatics

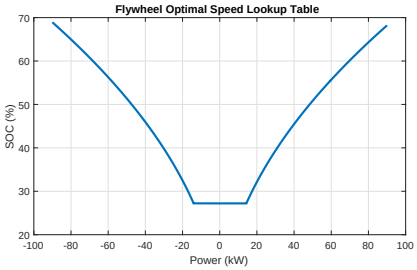

Figure 3: Lookup Table: optimal SOC vs flywheel output power.

$$J_{MPC} = \sum_{k=t}^{t+N_T T_s} L_{HESS_{MPC}}(k), \tag{12}$$

where

$$L_{HESS_{MPC}}(x(k),u(k)) = (1-\lambda)(P_{FL}(k) - P_B(k) - P_{FW}(k))^2 + \lambda(Loss_B(k) + Loss_{FW}(k)) + \gamma(x_2(k) - SOC_{FW_d})^2; \tag{13}$$

subject to the constraints (8) and (9). By varying γ, we are able to obtain the best achievable solution. In this study, γ is tuned off-line. How to plan the flywheel SOC reference (i.e., SOC_{FW_d}) to achieve accurate power tracking and efficient energy management is the major focus of this paper.

The flywheel optimal SOC reference highly depends on the load. The optimal SOC reference at different sea states (SS) varies significantly. For example, the SOC reference of flywheel could vary from 25% to 70%. Due to the high-frequency nature of the load fluctuations, the instantaneous power cannot be used directly to determine the optimal SOC. Therefore, the future power prediction from the MPC is very important. For the B/FW HESS, compared to flywheel energy storage alone, the power split between the battery and flywheel is another important factor that affects the optimal SOC reference of the flywheel. The battery and flywheel jointly compensate the load fluctuations, so the SOC reference of the flywheel cannot be obtained without the knowledge of the power split. Due to the computational cost of MPC, a long predictive horizon is almost impossible for this application, since the sampling time is small. Therefore, an SOC-reference approach must take advantage of the information available over a short predictive horizon. A detailed analysis of stability, though important and interesting, is not in the scope of this paper. To stabilize the MPC, one of the following two approaches is usually adopted [38]. One is to include the terminal cost and constraints in the MPC formulation, while the other is to have a sufficiently large horizon. In this paper, the first approach is adopted.

III. Planning Flywheel Reference SOC

In this paper, we develop two different approaches to find the flywheel reference SOC: a lookup-table-based approach and an optimization-based approach. The lookup-table based approach is determined by minimizing the flywheel losses:

$$J_{FW_{Loss}} = Loss_{FW}, \tag{14}$$

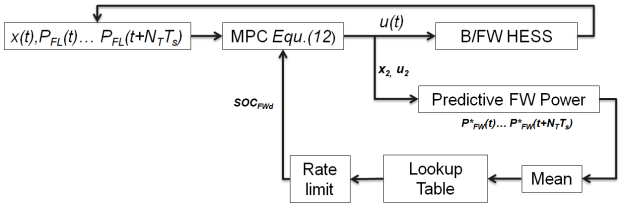

Figure 4: Lookup Table: Mean Power.

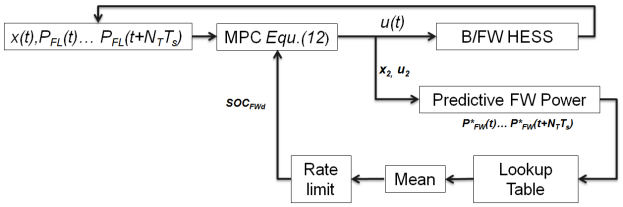

Figure 5: Lookup Table: Mean Speed

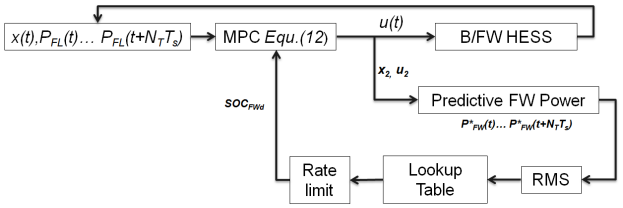

Figure 6: Lookup Table: RMS Power.

subject to the constraints:

$$P_{FW} = N_{FW}\omega_{max} SOC_{FW} T_{FW} - Loss_{FW}, \tag{15}$$

and the physical constraints in (8). The resulting lookup table is shown in Fig. 3. When implementing the lookup table, there are several approaches:

- Mean-value based approach;
- Instantaneous-power based approach;
- RMS-value based approach.

The approach in [17], where the mean value of the future power is used as the input of the lookup table, is labeled as "Mean Power", as shown in Fig. 4. However, the mean power does not represent the fluctuating power. Therefore, a second lookup-table based approach uses all the future load powers from MPC as inputs to the lookup table. Instead of a single SOC reference, the lookup table provides a sequence of SOC references based on instantaneous power. However, this approach does not take the flywheel dynamics into consideration. Therefore, the mean value of these SOC references is used as the final SOC reference , as shown in Fig. 5. This approach is labeled as "Mean Speed". These two approaches serve as the baseline approaches.

To capture the effects of load fluctuations, the RMS value of the predicted power is used as an input to the lookup table in the third approach, as shown in Fig. 6. This approach is labeled as "RMS Power".

Besides the lookup-table based approaches, an optimization-based approach is developed as well, as shown in Fig. 7. This approach minimizes the flywheel losses with the same output

This article has been accepted for publication in a future issue of this journal, but has not been fully edited. Content may change prior to final publication. Citation information: DOI 10.1109/TII.2020.2973409, IEEE Transactions on Industrial Informatics

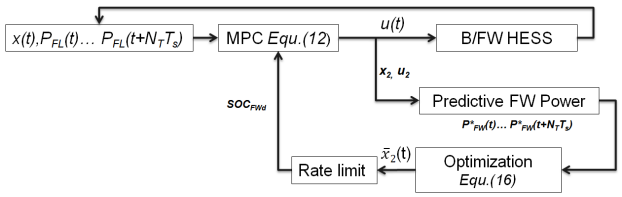

Figure 7: Optimization-based approach.

power as the MPC output power. The problem formulation is presented in the following:

$$J_{OPT}(S\bar{O}C_{FW}(k),\bar{T}_{FW}(k)) = \sum_{k=t}^{t+N_T T_s} Loss_{FW}(k), \qquad (16)$$

subject to the constraints:

$$P^*_{FW}(k) = N_{FW} \times (\omega_{max} S\bar{O}C_{FW}(k)\bar{T}_{FW}(k) - Loss_{FW}(k)), \quad (17)$$

the flywheel physical constraints in (8), and the flywheel dynamics constraint in (9), where $P^*_{FW}(t), P^*_{FW}(t+T_s)...P^*_{FW}(t+N_T T_s)$ are the flywheel output power based on the MPC optimized control sequence $u^*(t)$, $u^*(t+T_s)$, ..., $u^*(t+N_T T_s)$ and the initial state $SOC_{FW}(t)$. Note that to distinguish the optimization problem in MPC, $S\bar{O}C_{FW}$ and $\bar{T}_{FW}$ are used in this optimization-based approach. This approach aims to provide a state variable for the SOC reference. The difference between (14) and (16) is that the flywheel dynamic constraint is considered in (16), and (14) is only based on the instantaneous power.

IV. Performance Evaluation and Discussion

In this section, case studies are performed for an electric cargo ship. The performance of the proposed HESS control strategies is presented and analyzed through case studies.

A. Key Parameters of Case Studies

The size of the HESS is determined, according to the frequency characteristics of the power fluctuations. To quantitatively analyze the performance, three sea states, corresponding to smooth (sea state 2), moderate (sea state 4), and severe (sea state 6) operating conditions, are used in the simulation and analysis. Key parameters used in the simulation are shown in Tables II and III. A Li-ion battery module (BATVXLFP 100 Ah) and a high-speed flywheel module (Vycon) are used in this study. The nominal voltage of one battery module is 128 V, and its maximum current is 300 A. A maximum charge/discharge power of the flywheel is 90 kW and its maximum rotational speed is as high as 36,750 rpm. The three-phase permanent magnet machine is used as the motor/generator for this Vycon flywheel.

In this paper, the HESS sizing is designed based on an energy and power requirement analysis of load fluctuations at nominal sea state (SS4), as shown in Table IV. According to the aforementioned requirements and the frequency characteristics of the load power, the size of the HESS is selected as $N_B = 6$ and $N_{FW} = 3$, with the assumed operating condition: $I_B = 150A$, $T_{FW} = 30N$, $SOC_B = 80\%$, and $SOC_{FW} = 80\%$.

Table II: Key parameters.

Description	Value
Ship length	$190m$
Ship breadth	$28.4m$
Draft	$15.8m$
Mass	$20000ton$
Added-mass	$28755ton$
Thrust deduction coefficient	0.2
Propeller diameter	$5.6m$
Wetted area	$12297m^2$
Advance facing area in the air	$675.2m^2$
Water resistance coefficients	0.0043
Air resistance coefficient	0.8
Wave period	12sec
Wave height	0.5m(SS2)/ 2m(SS4)/ 4m(SS6)
Wave length	40.29% ship length
Ship speed command	12.4 knot
Motor speed command	125 rpm

Table III: B/FW hybrid energy storage parameters.

Description	Parameter	Value
Battery ESR resistance	R_B	$64m\Omega$
Flywheel maximum speed	ω_{max}	$36750rmp$
Flywheel stator resistance	R_s	$6m\Omega$
Flywheel inertia	J_{FW}	$0.6546kgm^2$

The control-oriented battery model is based on the equivalent series resistance model, as discussed in Section II. The simulation-oriented battery model uses the first-order equivalent circuit model (an ohmic resistance with an RC pair). The parameter identification results, as shown in Fig. **??**, are used to evaluate the performance of the proposed strategies.

B. Simulation Results of Case Studies

Three performance metrics over the 40 minutes of the self-sustained operation period are defined in the following:

1) RMS tracking error: $\sqrt{J_1/(N_T T_s)}$;
2) HESS losses: $Loss\% = \frac{J_2}{\sum_{k=t}^{N_T T_s} P_{FL}(k)} \times 100\%$;
3) Loss difference: $Loss_{diff}\% = \frac{Loss_1 - Loss_2}{Loss_2} \times 100\%$.

The first two performance metrics are used for determining the Pareto fronts, and the third represents the HESS losses difference between two approaches with the same RMS tracking error; $Loss_1$ and $Loss_2$ represent the HESS losses of the first and second approaches, respectively, and the one with the larger losses is defined as the first approach. The optimization problem (7) - (9) is solved by dynamic programming to provide the global optimal solution, which can be characterized in three phases: initial, steady, and final operation, as shown in Fig. 2. In the initial phase, regardless of the initial SOC, the flywheel SOC converges to the same range, which is the high-efficiency range for the given load fluctuations. The flywheel operates within this high-efficiency range until it reaches the final phase. The behavior in the final phase is similar to the short predictive horizon MPC without SOC reference. As shown in Fig. 2, the optimal SOC reference is around 55%.

The main results and key observations are summarized in the following remarks:

Remark 4.1 (Reference SOC): As shown in Fig. 8, with different initial SOCs (i.e., 80%, 55%, and 40%) and the

This article has been accepted for publication in a future issue of this journal, but has not been fully edited. Content may change prior to final publication. Citation information: DOI 10.1109/TII.2020.2973409, IEEE Transactions on Industrial Informatics

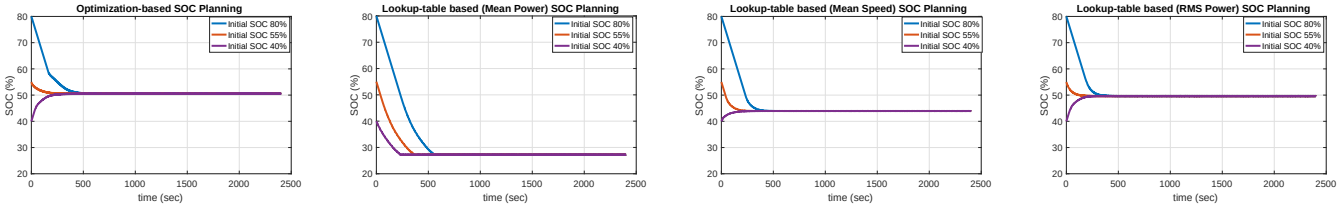

Figure 8: SOC reference with different initial SOCs at sea state 4.

Table IV: Power and energy requirements at sea state 4.

	Low Frequency	High Frequency	Total
Maximum Power	114kW	194kW	308kW
Energy Storage	121Wh	2.05Wh	123Wh

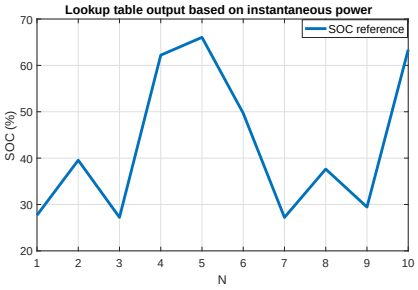

Figure 9: Lookup output based on instantaneous power.

same γ, the convergence of the SOC reference represents the effectiveness of each approach. The baseline approach, namely "Mean Power", has the largest difference from the global optimal SOC (55%), as shown in Fig. 2. The reason is that the average value of power fluctuation cannot represent the fluctuation power condition. The average value could be zero, even though the amplitude of the fluctuations is large. The "Mean Speed" can capture all the instantaneous power of load fluctuations. However, the flywheel dynamic is ignored, resulting in large variations of SOC references ($SOC_{ref}(k)$, $SOC_{ref}(k+T_s)$,...,$SOC_{ref}(k+N_TT_s)$), as shown in Fig. 9. The average value of ($SOC_{ref}(k), SOC_{ref}(k+Ts), ..., SOC_{ref}(k+N_TT_s)$) still significantly differs from the optimal SOC reference. The proposed "RMS Power" approach has the best performance among all three lookup-table based approaches, because it represents the power load fluctuations. As shown in Fig. 8, the SOC reference of "RMS Power" is around 49%. The optimization-based approach achieves a reference SOC of 51%, which is very close to the optimal SOC reference, as shown in Fig. 2.

Remark 4.2 (Pareto fronts): Varying the weighting factor λ allows us to put a different relative emphasis on each attribute to investigate performance tradeoffs (i.e., the Pareto front). The Pareto fronts provide insights into the tradeoff between accurate tracking and efficient operation for different approaches. Different initial SOCs of the flywheel are taken into consideration at the nominal sea state (SS4). As shown in Fig. 10, the optimization-based approach achieves the best performance. The "RMS Power" approach also achieves very impressive performance, and the results in Fig. 10 match the analysis in Remark 4.1. At low sea state, i.e., SS2, the difference between the optimization-base approach and the "RMS Power" approach is smaller than that at SS4 or SS6. At high sea state, i.e., SS6, the "Mean Power" has better performance than "Mean Speed". The reason is that the flywheel is operating at its max power over a much longer time than that at SS2 or SS4. When the flywheel is always working at its max power, the mean value is close to the RMS value. According to the performance metric $Loss_{diff}\%$, as compared to the baseline approach using the "Mean Power", the proposed optimization-based approach can achieve an HESS loss reduction of 130%, 63.4%, and 58.6% at sea states 4, 2 and 6, respectively. This comparison also shows the importance of flywheel SOC planning.

Remark 4.3 (Optimization vs. lookup table): "RMS Power" is the best lookup-table based approach, whose performance is very close to the optimization-based approach. Compared to "RMS Power", the optimization-based approach can achieve a 2% to 5% reduction in losses with the same tracking error at nominal and high sea states. However, the computational cost of the optimization-based approach is much higher than the lookup-table based approach. The computational cost highly depends on the controller hardware, optimization solver, predictive horizon, and initial value. Since the proposed approaches focus on a short predictive horizon and the initial value can be obtained by "RMS Power", the controller hardware and optimization solver are the major factors to decide whether or not the optimization-based approach is possible. In this study, Sequential Quadratic Programming (SQP) is used to solve the optimization problem in the simulation. In general, when the controller hardware capability is limited, the lookup-table-based approach, namely "RMS Power", is the preferred solution, since it can achieve comparable performance with low computational complexity. On the other hand, if the controller hardware capability is sufficient, then the proposed optimization-based approach is still the best solution.

The simulation results studied above are based on accurate predictive load fluctuations. It is important to evaluate the performance with uncertainties in the prediction. In general, the predictive accuracy decreases as the predictive horizon increases. In this paper, a short predictive horizon is used to avoid significant errors in prediction. Random predictive errors (up to 10% of the predictive load fluctuation) are added into the future load prediction ($P_{FL}(t+T_s), ..., P_{FL}(t+N_TT_s)$) at sea state 4. Since the instantaneous load fluctuation $P_{FL}(t)$ is measurable, no error is added into this term. The Pareto fronts of the proposed two strategies with and without predictive uncertainties are shown in Fig. 11. The simulation results show that the proposed algorithms are still effective even when

This article has been accepted for publication in a future issue of this journal, but has not been fully edited. Content may change prior to final publication. Citation information: DOI 10.1109/TII.2020.2973409, IEEE Transactions on Industrial Informatics

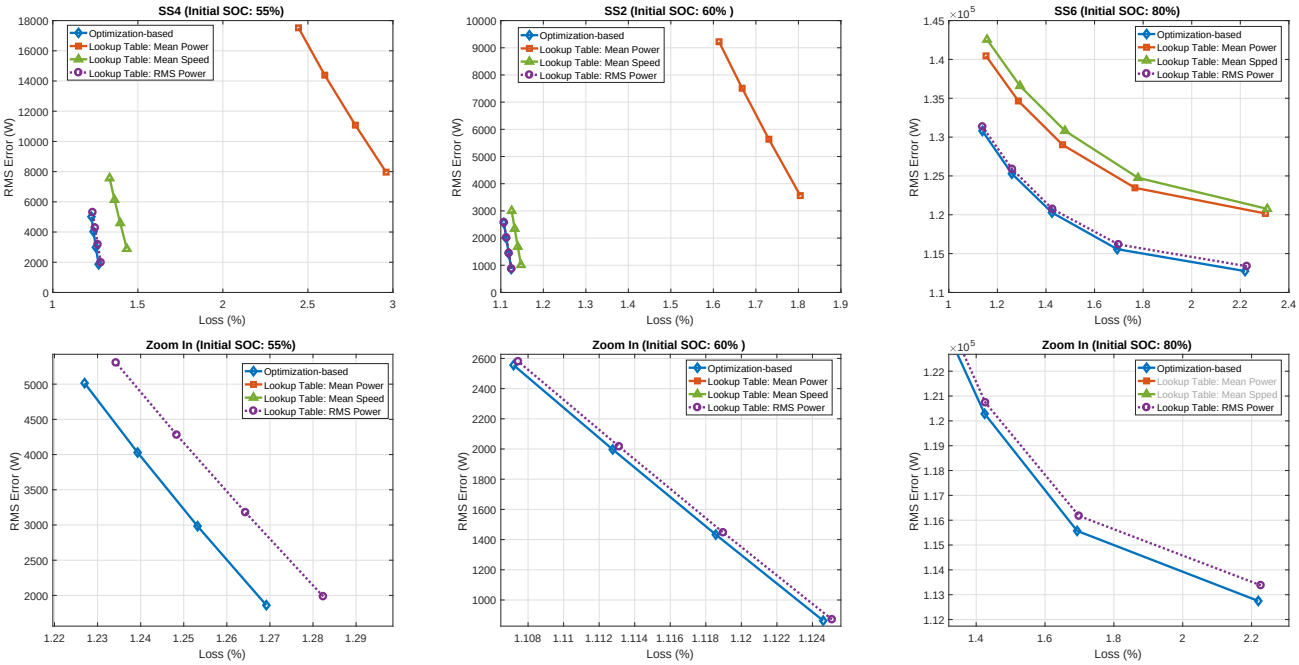

Figure 10: Performance comparison: Pareto fronts of different approaches at sea states 4, 2 and 6.

including random predictive errors.

As discussed in Section II, the RC model, in general, can capture the battery dynamics more accurate than the ESR model, but the RC pair has only a slight influence on the MPC performance in this application. In order to show the differences between the RC model and ESR model, a simulation study is performed. As shown in Fig. 12, the performance of the more accurate model ($R0+RC$) is slightly better than that of the simplified model (ESR) for the same energy management strategy. The differences become even ignorable for the proposed approaches, compared to the baseline approaches. Given the increased computational complexity of the RC model, it is reasonable to use the ESR model in this application. Furthermore, the proposed approaches with the ESR model still outperform the baseline approaches with the RC model, which demonstrates the importance of a proper energy management strategy.

C. Hardware-in-the-loop Test

In order to evaluate the real-time feasibility of the proposed MPC approach, a hardware-in-the-loop (HIL) test is performed. As shown in Fig. 13, the Speedgoat control system, which has an Intel Core i5-680 3.6GHz processor with a 320GB SATA hard disk main drive and a 4096MB DDR3 memory, is used in this HIL test. The proposed "RMS Power" approach is tested by using the Integrated Perturbation Analysis and Sequential Quadratic Programming (IPA-SQP) algorithm. This solver estimates the optimal solution using a combination of prediction and correction. In IPA-SQP, a perturbation analysis approximates an optimal solution in the prediction step, and the solution is corrected by SQP if the approximated solution is larger than the tolerance. The maximum execution time of the "RMS Power" approach is 6.8722×10^{-5} seconds, while the average execution time is 4.4876×10^{-5} seconds. The task execution time represents the computational time of the proposed algorithm at each sample step. Both the maximum and average execution time are smaller than the sample time (0.02 seconds), which demonstrates the real-time feasibility of the proposed approach. The battery and flywheel outputs in the HIL test are shown in Fig. 14. Note that the Pareto fronts, which are calculated in offline simulations, aim to provide insight into the tradeoffs between accurate tracking and efficient operation. The HIL test herein is only one single point in the Pareto front to evaluate the computational time.

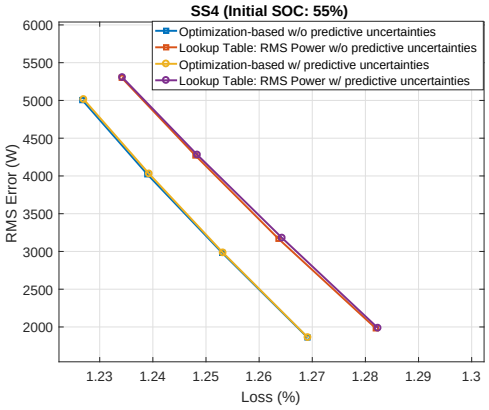

Figure 11: Pareto fronts of the proposed two strategies with and without predictive uncertainties.

V. CONCLUSIONS

In this paper, a battery with flywheel (B/FW) hybrid energy storage system which compensates load fluctuations in shipboard microgrids is investigated, leading to improved system

This article has been accepted for publication in a future issue of this journal, but has not been fully edited. Content may change prior to final publication. Citation information: DOI 10.1109/TII.2020.2973409, IEEE Transactions on Industrial Informatics

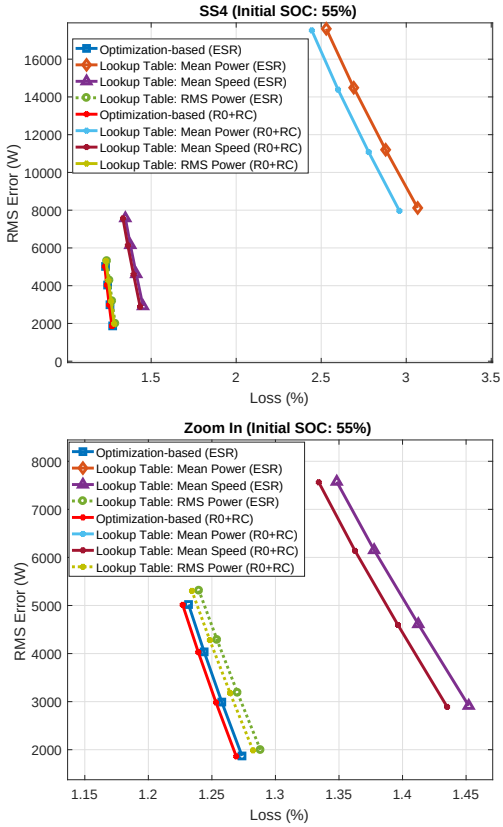

Figure 12: Differences between the ESR model and the RC model.

Figure 13: The real-time controller used in the HIL test.

efficiency and enhanced power reliability. The control strategy, which integrates model predictive control (MPC) and flywheel SOC reference planning, is developed to minimize the power tracking error and HESS losses. In order to find the flywheel SOC reference, both lookup-table-based and optimization-based approaches are developed. Simulation results at different sea conditions, namely sea states 2, 4 and 6, demonstrate the effectiveness of the proposed approaches. The lookup-table based approach, which uses the RMS value of power fluctuations as the input of the lookup table, achieves comparable performance to the optimization-based approach, but with a substantial lower computational complexity. It is therefore a preferred approach particular for applications with limited computation resources. If the controller hardware capability is sufficient, the proposed optimization-based approach is the best option.

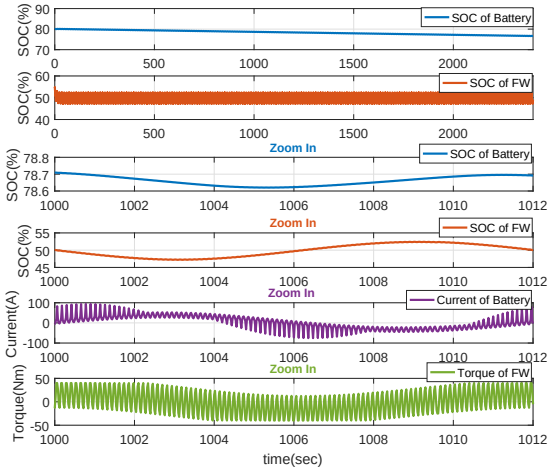

Figure 14: Battery and Flywheel outputs in the HIL test.

REFERENCES

[1] P. Sanjeev, N.P. Padhy, and P. Agarwal, "Autonomous power control and management between standalone DC microgrids". *IEEE Transactions on Industrial Informatics*, vol. 14, no. 7, pp.2941-2950, 2018.

[2] G. Dong, and Z. Chen, "Data-Driven energy management in a home microgrid based on Bayesian optimal algorithm". *IEEE Transactions on Industrial Informatics*, vol. 15, no. 2, pp.869-877, 2019.

[3] F. Luo, et al., "Multiagent-based cooperative control framework for microgrids' energy imbalance". *IEEE Transactions on Industrial Informatics*, vol. 13, no. 3, pp.1046-1056, 2017.

[4] K. Jia, et al., "Historical-data-based energy management in a microgrid with a hybrid energy storage system". *IEEE Transactions on Industrial Informatics*, vol. 13, no. 5, pp.2597-2605, 2017.

[5] J. Hou, J. Sun and H. Hofmann, "Adaptive model predictive control with propulsion load estimation and prediction for all-electric ship energy management", *Energy*, vol. 150, pp. 877-889, 2018.

[6] D. Wang, et al., "A demand response and battery storage coordination algorithm for providing microgrid tie-line smoothing services". *IEEE Transactions on Sustainable Energy*, vol. 5, no. 2, pp.476-486, 2014.

[7] Z. Song, et al., "Parameter Identification and Maximum Power Estimation of Battery/Supercapacitor Hybrid Energy Storage System Based on Cramer-Rao Bound Analysis." *IEEE Transactions on Power Electronics* 34, no. 5 (2019): 4831-4843.

[8] L. He, et al., "A Flexible Power Control Strategy for Hybrid AC/DC Zones of Shipboard Power System With Distributed Energy Storages". *IEEE Transactions on Industrial Informatics*, vol. 14, no. 12, pp.5496-5508, 2018.

[9] Z. Jin, L. Meng, J.M. Guerrero, and R. Han, "Hierarchical control design for a shipboard power system with DC distribution and energy storage aboard future more-electric ships". *IEEE Transactions on Industrial Informatics*, vol. 14, no. 2, pp.703-714, 2018.

[10] T. J. McCoy, "Electric ships past, present, and future". *IEEE Electrification Magazine*, vol. 3, no. 2, pp. 4-11, 2015.

[11] N. Doerry, J. Amy, and C. Krolick, "History and the status of electric ship propulsion, integrated power systems, and future trends in the us navy." *Proceedings of the IEEE*, vol. 103, no. 12, pp: 2243-2251, 2015.

[12] Ø. N. Smogeli and A. J. Sørensen, "Antispin thruster control for ships," *IEEE Transactions on Control Systems Technology*, vol. 17, no. 6, pp. 1362–1375, 2009.

[13] T.I. Bø, and T.A. Johansen, "Battery power smoothing control in a marine electric power plant using nonlinear model predictive control". *IEEE Transactions on Control Systems Technology*, vol. 25, no. 4, pp.1449-1456, 2017.

[14] J. Hou, J. Sun and H. Hofmann, "Mitigating power fluctuations in electric ship propulsion with hybrid energy storage system: design and analysis", *IEEE Journal of Oceanic Engineering*, vol. 43, no. 1, pp. 93-107, 2018.

[15] R.E. Hebner, et al., "Dynamic load and storage integration", *Proceedings of the IEEE*, vol. 103, no. 12, pp.2344-2354, 2015.

[16] J.D Park, C. Kalev and H. Hofmann, "Control of high-speed solid-rotor synchronous reluctance motor/generator for flywheel-based uninterruptible power supplies". *IEEE Transactions on Industrial Electronics*, vol. 55, no. 8, pp.3038-3046, 2008.

[17] F. Díaz-González, A. Sumper, O. Gomis-Bellmunt and F.D. Bianchi, "Energy management of flywheel-based energy storage device for wind power smoothing". *Applied Energy*, vol. 110, pp.207-219, 2013.

[18] M. Cheng, S.S. Sami and J. Wu, "Benefits of using virtual energy storage system for power system frequency response". *Applied Energy*, vol. 194, pp.376-385, 2017.

[19] B. Bolund, H. Bernhoff and M. Leijon, "Flywheel energy and power storage systems". *Renewable and Sustainable Energy Reviews*, vol. 11, no. 2, pp.235-258, 2007.

[20] J. Kuseian, "Naval power system technology development roadmap", Electric Ships Office, PMS 320, 2013.

[21] H. He, H. Jia, C. Sun, and F. Sun, "Stochastic Model Predictive Control of Air Conditioning System for Electric Vehicles: Sensitivity Study, Comparison, and Improvement", *IEEE Transactions on Industrial Informatics*, vol. 14, no. 9, pp. 4179 - 4189, 2018.

[22] S. Feng, H. Sun, Y. Zhang, J. Zheng, H. X. Liu, and L. Li. "Tube-based discrete controller design for vehicle platoons subject to disturbances and saturation constraints." *IEEE Transactions on Control Systems Technology* (2019).

[23] X. Luo, J. Wang, M. Dooner, and J. Clarke. "Overview of current development in electrical energy storage technologies and the application potential in power system operation." Applied energy 137 (2015): 511-536.

[24] X. Tang, Y. Wang, C. Zou, K. Yao, Y. Xia, and F. Gao. "A novel framework for Lithium-ion battery modeling considering uncertainties of temperature and aging." Energy conversion and management 180 (2019): 162-170.

[25] W. Waag, S. Kabitz, and D. Uwe Sauer. "Experimental investigation of the lithium-ion battery impedance characteristic at various conditions and aging states and its influence on the application." Applied energy 102 (2013): 885-897.

[26] Y. Wang, X. Zhang, C. Liu, R. Pan, and Z. Chen. "Multi-timescale power and energy assessment of lithium-ion battery and supercapacitor hybrid system using extended Kalman filter." Journal of Power Sources 389 (2018): 93-105.

[27] F. Zhang, X. Hu, R. Langari, and D. Cao. "Energy management strategies of connected HEVs and PHEVs: Recent progress and outlook." *Progress in Energy and Combustion Science* 73 (2019): 235-256.

[28] S. Feng, X. Wang, H. Sun, Y. Zhang, and L. Li. "A better understanding of long-range temporal dependence of traffic flow time series." *Physica A: Statistical Mechanics and its Applications* 492 (2018): 639-650.

[29] J. Hou, J. Sun and H. Hofmann, "Control development and performance evaluation for battery/flywheel hybrid energy storage solutions to mitigate load fluctuations in all-electric ship propulsion systems", *Applied Energy*, vol. 212, pp. 919-930, 2018.

[30] X. Hu, H. Jiang, F. Feng, and B. Liu. "An enhanced multi-state estimation hierarchy for advanced lithium-ion battery management." *Applied Energy* 257 (2020): 114019.

[31] M. Ye, Min, H. Guo, R. Xiong, and Q. Yu. "A double-scale and adaptive particle filter-based online parameter and state of charge estimation method for lithium-ion batteries." *Energy* 144 (2018): 789-799.

[32] F. Sun and R. Xiong. "A novel dual-scale cell state-of-charge estimation approach for series-connected battery pack used in electric vehicles." *Journal of Power Sources* 274 (2015): 582-594.

[33] T. Feng, L. Yang, X. Zhao, H. Zhang, and J. Qiang. "Online identification of lithium-ion battery parameters based on an improved equivalent-circuit model and its implementation on battery state-of-power prediction." *Journal of Power Sources* 281 (2015): 192-203.

[34] Z. Song, et al. "Combined State and Parameter Estimation of Lithium-Ion Battery with Active Current Injection." *IEEE Transactions on Power Electronics* (2020).

[35] C. Zou, et al., "A review of fractional-order techniques applied to lithium-ion batteries, lead-acid batteries, and supercapacitors". *Journal of Power Sources*, vol. 390, pp.286-296, 2018.

[36] R.T. Doucette and M.D. McCulloch "A comparison of high-speed flywheel, batteries, and ultracapacitors on the bases of cost and fuel economy as the energy storage system in a fuel cell based hybrid electric vehicle". *Journal of Power Sources*, vol. 196, no. 3, pp.1163-1170, 2011.

[37] J. Sun, "Optimisation-based control for electrified vehicles: challenges and opportunities". *Journal of Control and Decision*, vol. 2, no. 1, pp.46-63, 2015.

[38] D. Mayne and P. Falugi. "Generalized stabilizing conditions for model predictive control." *Journal of Optimization Theory and Applications* 169, no. 3 (2016): 719-734.

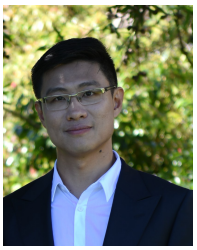

Jun Hou (S'15-M'18) received his Ph. D degree from the University of Michigan, Ann Arbor in 2017, and his M.S. degrees in electrical engineering from Northeastern University, China, in 2011. His current research interests include integration, modeling, control, and optimization of hybrid energy storage, power electronic converters and electric propulsion systems. Dr. Hou is the author or co-author of more than 30 peer-reviewed publications including more than 20 journal articles. Dr. Hou is a reviewer of over 20 SCI journals with over 200 reviewed articles. He has been awarded "Outstanding Reviewer Awards" by Applied Energy and Energy, "Global Peer Reviewer Awards" by Pulbons, and the "Fifth National Youth Technological Innovative Award" in the Great Hall of the People, China.

Ziyou Song (M'18) received his B.E. degree (with honor) and Ph.D. degree (with highest honor and thesis award) in Automotive Engineering from Tsinghua University, Beijing, China, in 2011 and 2016, respectively. He worked as a research scientist at Tsinghua University from 2016 to 2017 and is currently a Postdoctoral Research Fellow in the Department of Naval Architecture and Marine Engineering, and Department of Electrical Engineering and Computer Science, at the University of Michigan, Ann Arbor. His research interests lie in the areas of modeling, estimation, optimization, and control of energy storage for electrified vehicles and renewable systems. Dr. Song is the author or co-author of more than 50 peer-reviewed publications including more than 40 journal articles. He has received several paper awards, including Applied Energy 2015-2016 Highly Cited Paper Award, Applied Energy Award for Most Cited Energy Article from China, NSK Outstanding Paper Award of Mechanical Engineering, and 2013 IEEE VPPC Best Student Paper Award.

Heath F. Hofmann (S'90-M'92-SM'16) received the Ph.D. degree in electrical engineering and computer science from the University of California at Berkeley, Berkeley, CA, USA, in 1998. He is currently a Professor with the University of Michigan, Ann Arbor, MI, USA. He has authored approximately four dozen papers in refereed journals. He currently holds 14 patents. His research interests include power electronics, specializing in the design, simulation, and control of electromechanical systems, adaptive control techniques, energy harvesting, flywheel energy storage systems, electric and hybrid electric vehicles, and finite-element analysis.

Jing Sun (M'89-SM'00-F'04) received her Ph.D. degree from University of Southern California in 1989, and her B.S. and M.S. degrees from University of Science and Technology of China in 1982 and 1984 respectively. From 1989-1993, she was an assistant professor in Electrical and Computer Engineering Department, Wayne State University. She joined Ford Research Laboratory in 1993 where she worked in the Powertrain Control Systems Department. After spending almost 10 years in industry, she came back to academia and joined the faculty of the College of Engineering at the University of Michigan in 2003, where she is now Michael G. Parsons Professor and the chair in the Department of Naval Architecture and Marine Engineering, with courtesy appointments as a professor in the Department of Electrical Engineering and Computer Science and Department of Mechanical Engineering. Her research interests include system and control theory and its applications to marine and automotive propulsion systems. She holds 39 US patents and has co-authored a textbook on Robust Adaptive Control. She is an IEEE Fellow and a recipient of the 2003 IEEE Control System Technology Award.